

## A STUDY ON SEISMIC SSI ANALYSIS FOR RB COMPLEX ON PILES INCLUDING THE EFFECTS OF MOTION INCOHERENCY AND SOIL NONLINEAR BEHAVIOUR IN VICINITY OF PILES

Dan M. Ghiocel<sup>1</sup>, Yalcin Bulut<sup>2</sup>

<sup>1</sup> Chief of Engineering, Ghiocel Predictive Technologies, Inc., NY, USA (dan.ghiocel@ghiocel-tech.com)

<sup>2</sup> Managing Director, MATRISeb, Ankara, Turkey (ybulut@matriseb.com)

### ABSTRACT

The paper investigates the SSI effects for a heavy building complex founded on concrete piles. The paper focuses on the effects of the local nonlinear soil behaviour in the vicinity of piles. Additionally, the effects of inclined SV-P waves and SH waves are included. The paper presents SSI result comparisons including ISRS, structural displacements, and pile forces and moments. Comparisons between seismic SSI results for the “without piles” and the “with piles” cases are included. The seismic SSI analysis is performed using the ACS SASSI software that can simulate incoherent random wavefields via an accurate Monte Carlo method implementation and include the local soil hysteretic behaviour using an efficient iterative equivalent-linearization numerical procedure. The SSI modelling captures accurately both the kinematic and inertial SSI effects. The paper provides useful insights on the pile foundation dynamic behaviour.

### DESCRIPTION OF THE INVESTIGATED PROBLEMS

The paper investigates the seismic SSI effects for a heavy building complex founded on concrete piles, as shown in Figure 1. The RB complex foundation area is about 250 ft x 300 ft. The RB basemat is taken at the grade level, basically sitting on the pile foundation with no embedment and direct contact with the soil.

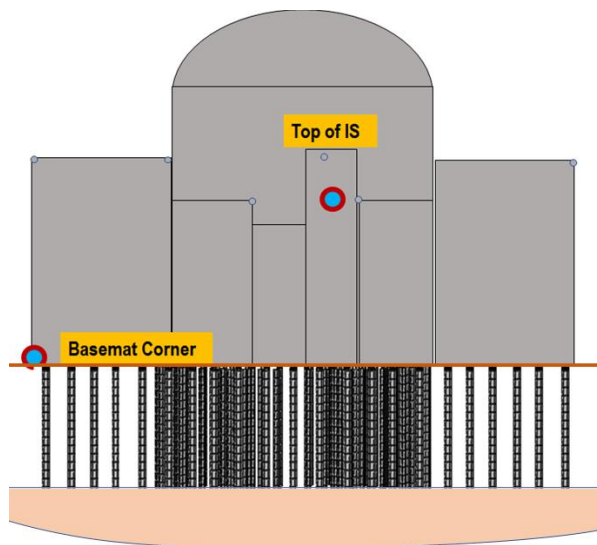


Figure 1. Nuclear Complex on Pile Foundation

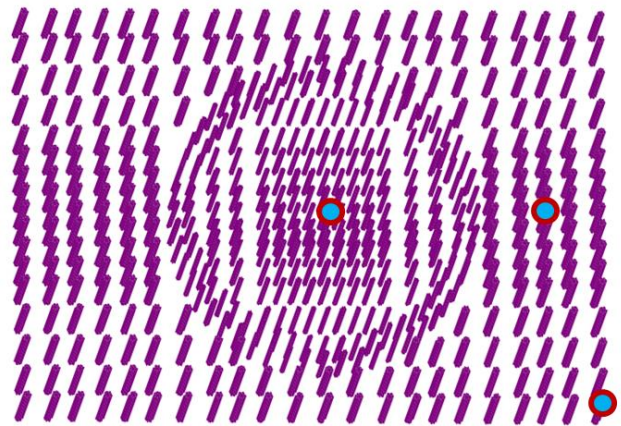


Figure 2. Pile Locations Under Basemat

The pile foundation depth is 60 ft below the grade level. Figure 2 shows the locations of the 495 concrete piles under the basemat. The concrete piles have either 3 ft or 4.5 ft diameter. The highest density of the concrete piles is under the containment structure as shown in Figure 2. The piles surrounding RB have larger spacings. The piles are peak-bearing piles which sitting on the rock formation at the 60 ft depth.

The soil deposit is shown in Figure 3 (blue line), include a soft soil layer of 60 ft thickness with a  $V_s$  varying between 750 fps and 900 fps above a rock formation with  $V_s$  of 5,500 fps. The seismic input is shown in Figure 4 and is defined at the ground surface by the European GRS for medium soil sites (black lines). The in-column SSI input motions for the horizontal and vertical directions are based on the spectrum-compatible acceleration motions generated based on the outcrop GRS at the at the top of rock formation of 60 ft depth which is assumed to be the same with the GRS at ground surface (red line). This procedure is based on the US practice for deep foundations that avoids performing surface motion deconvolution. The in-column FIRS or GRS computed at the rock formation depth is also shown in Figure 4 (with blue line). It should be noted that the large reduction of the GRS amplitudes is extremely drastic, and most like not acceptable for a real project, but acceptable herein for this research study.

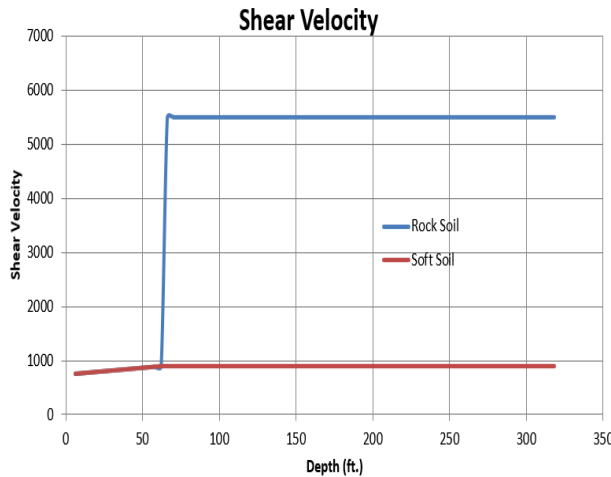


Figure 3. The Two  $V_s$  Soil Profiles Considered

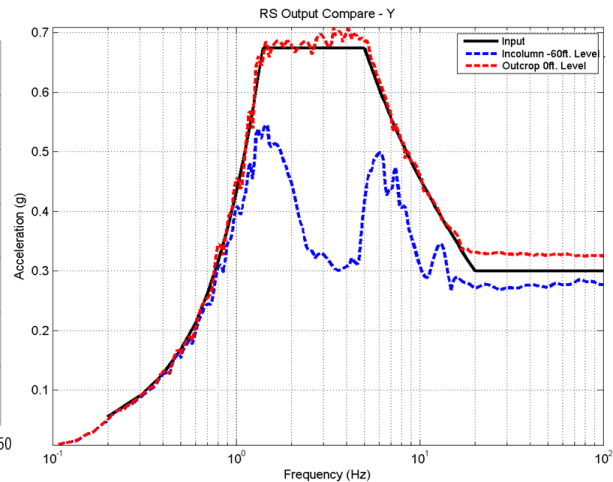


Figure 4. The GRS at the Pile Foundation Depth

For the incoherent SSI analysis, the ACS SASSI rigorous stochastic simulation approach (with no phase adjustment) was used. A set of 20 incoherent simulated wavefields were used to compute the (mean) incoherent SSI responses. The incoherency model was defined by the Abrahamson coherence function for soil sites (Abrahamson, 2007), including an apparent horizontal wave velocity of 4500 fps in X-longitudinal direction to simulate wave passage effects.

### ACS SASSI MODELING

The FE model mesh of the pile foundation part of the overall SSI model is shown in Figures 5 and 6. A total of about 228,000 nodes are included in the pile foundation model, not including the excavated soil nodes. The concrete piles with hexagonal cross-sections approximating the circular shape were modelled using linear-behaviour solid elements. Between the solid elements along the pile axis, soft beam elements are included, so that the pile forces and moments are easily extracted for comparisons of results. The adjacent soil and soil between piles is modelled by solid elements considered with either linear or nonlinear hysteretic behaviour based on the local soil strains. The FE mesh is sufficiently refined to provide reasonably accurate stresses and strains in the soil elements.

The RB complex building basemat is assumed with no embedment sitting only on the top of concrete piles. It was assumed that the basemat was not directly transmitting any pressure load to the surrounding soil. The seismic basemat forces and moments are transmitted to the concrete piles only. This SSI modelling avoids on purpose including the basemat contribution for computing the overall pile foundation impedance.

An important FE modelling aspect is related to the SASSI methodology is that the unstructured mesh for the inter-pile soil needs to be sufficiently refined, so that the soil element strains are accurately computed. At the same time, the excavated soil mesh should a regular structured mesh which can be coarser since the excavation volume includes a much more uniform soil material without any inserted piles. A transition mesh zone is needed to transition from the pile foundation refined mesh to the excavation coarser mesh at the common two lateral and bottom mesh boundaries.

The pile foundation SASSI FE modelling based on having a regular mesh for the excavated soil model is illustrated shown in Figures 5 and 6.

It should be noted that this SASSI modelling is recommended by the USNRC BNL consultants (Nie, Braveman and Costantino, 2013). This SSI modelling also provides an improved numerical efficiency. The entire SSI model of about a size of about 300,000 nodes was run on a 256 GB RAM PC workstation operating under MS Window 10 in less than 20 hours. Faster solutions for larger size problems can be obtained using the newer FVROM-INT approach (Ghiocel, 2022).

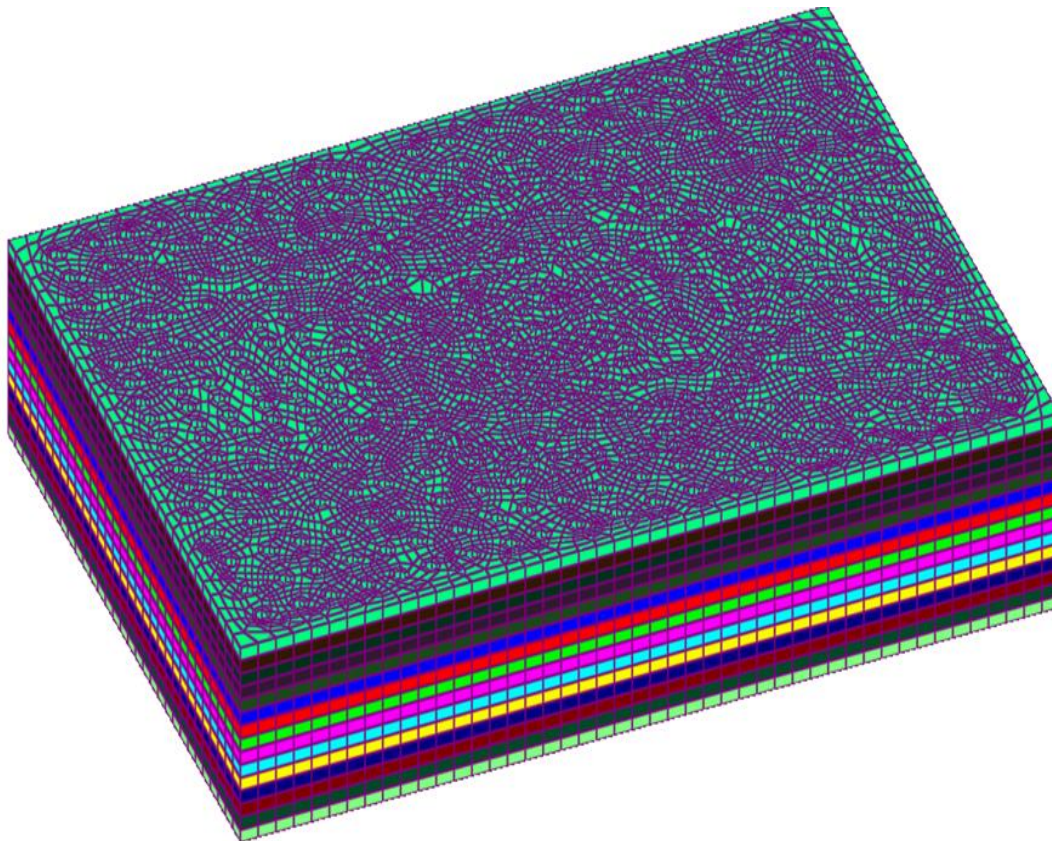


Figure 5. Pile Foundation Mesh Including All Embedment Soil Layer (about 228,000 nodes)

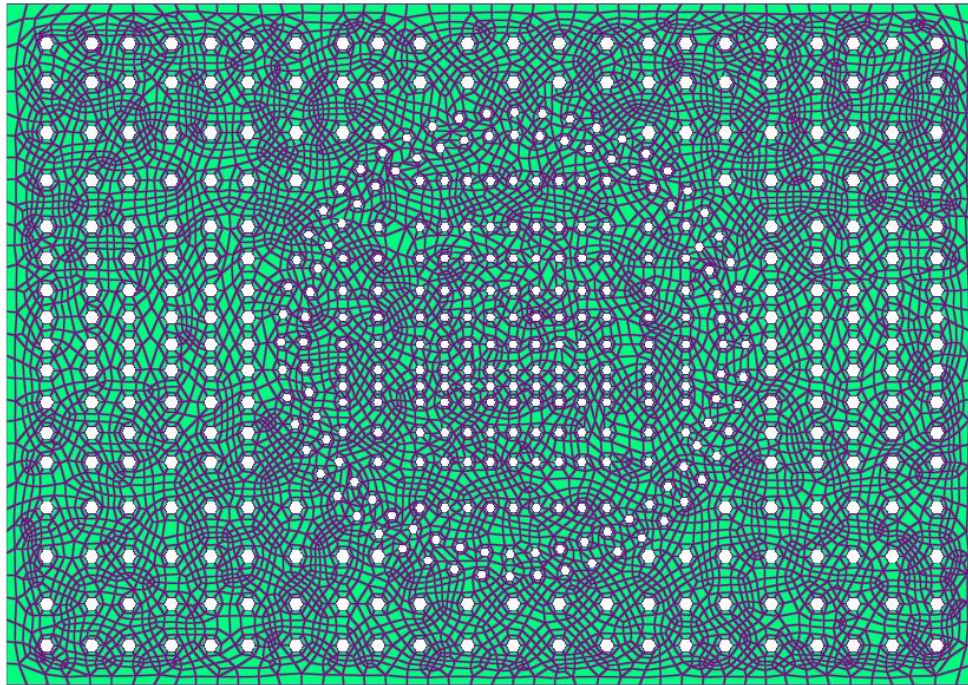


Figure 6. Pile Foundation Mesh at Each Embedment Soil Layer (about 12,000 nodes/layer)

### LINEARIZED SSI ANALYSIS RESULTS

In this section comparative SSI responses obtained are presented. Firstly, the comparative SSI results are presented between the cases “Without Piles” and “With Piles”. Firstly, we compare the SSI analysis results assuming a linear soil behaviour in the vicinity of the piles. Seismic input was defined by coherent motions.

Figure 7 shows the SSI relative displacement histories at the basemat corner of the RB complex in the Y transverse horizontal and Z vertical directions with respect to the basemat center motion. Figure 7 compares “Without piles” and “With piles” cases. The comparative SSI displacement results indicate a relatively weak influence of the piles for the basemat horizontal motion. As expected, for the vertical direction, the effect of piles is much larger. The basemat edge vertical displacements are drastically reduced by the effect of the peak-bearing piles by an order of magnitude. Basically, there is no basemat rocking for pile foundation.

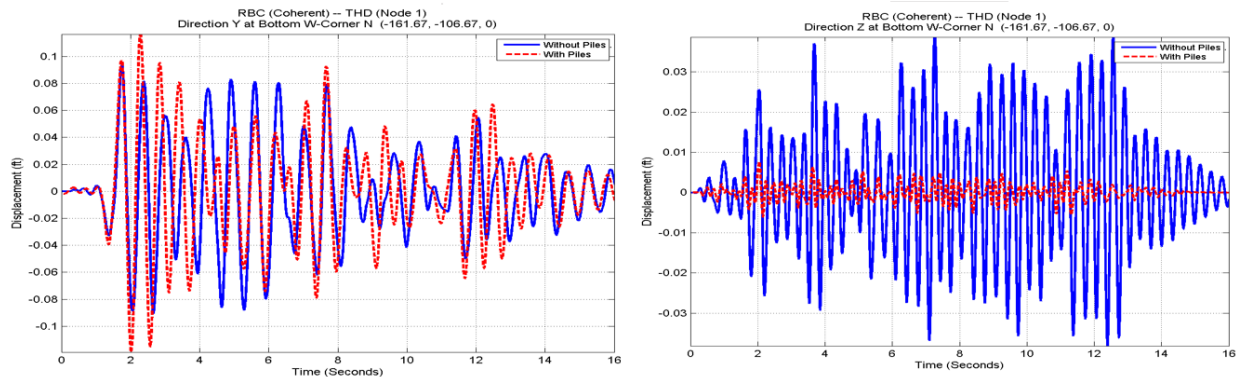


Figure 7. Basemat SSI Relative Displacement Response in Y-horizontal (left) and Z-vertical (right) directions for “With Piles” and “Without Piles”

Figures 8 and 9 show comparative ISRS computed at the basemat level for the Y and Z directions for the two cases, specifically, the peak-bearing piles and the floating-piles. The floating piles were simulated by assuming that there is no rock formation at 60 ft depth (Figure 3 red line). The plotted ISRS results include both the coherent and the incoherent ISRS for “With Piles” and “Without Piles”. The ISRS differences reflect same trends noticed for the SSI relative displacements.

It should be noted that the peak-bearing piles amplify by about 20% the horizontal ISRS peak near 1.9 Hz which corresponds to the largest SSI mode of the system in the horizontal direction. This ISRS amplification is a result of the decrease of the SSI effects due to the reduction of the SSI rocking motion at the basemat level due to the significant vertical stiffness introduced by the peak-bearing piles. The largest ISRS peak in the vertical direction @ 3.0 Hz is largely reduced by the peak-bearing piles. The effects of the motion incoherency on ISRS appear to be mild, being only significant in the vertical direction for the peak-bearing piles with up to 30% reduction of ISRS peaks. For the floating piles, the minor increase of the ISRS peak around 1.5 Hz in horizontal direction at basemat corner is due to the torsion produced by incoherency.

The ISRS result trends shown in Figures 8 and 9 should be quite general for the heavy buildings on floating piles or peak-bearing piles.

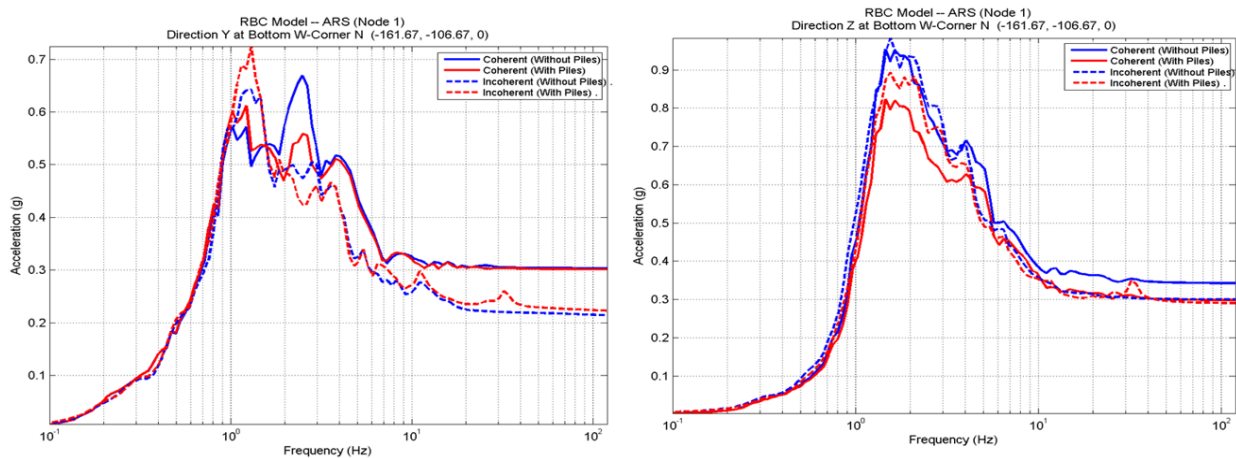


Figure 8 Floating Piles: Coherent & Incoherent ISRS in Y & Z dirs; “With Piles” vs. “Without Piles”

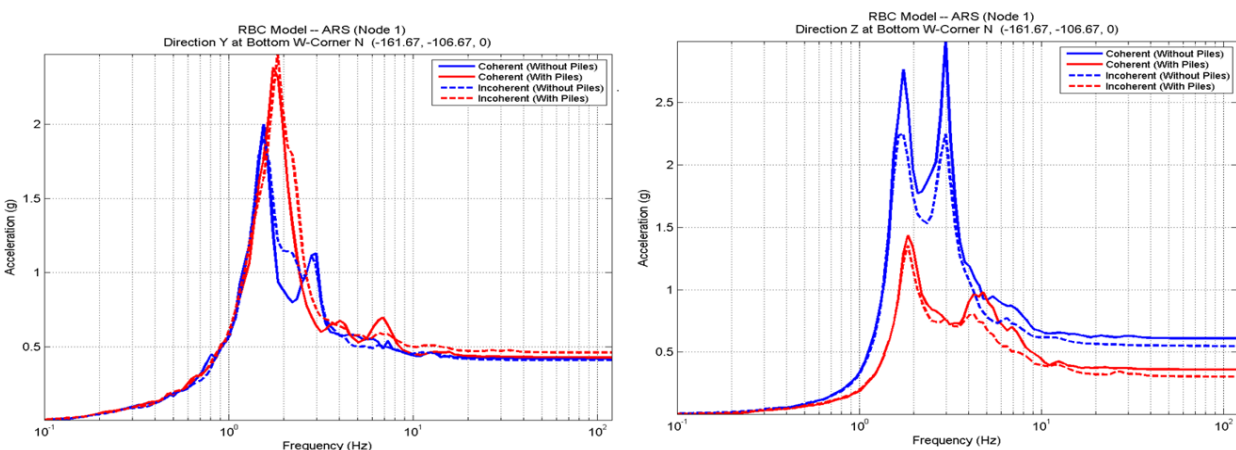


Figure 9 Peak Bearing Piles: Coherent & Incoherent ISRS in Y & Z dirs; “With Piles” vs. “Without Piles”

Figure 10 shows the effects of the motion incoherency on the axial forces and bending moments in the peak-bearing piles. The selected pile location is at the corner of the pile foundation as indicated in Figure 2 (see the marked low-right corner pile, in Group 57, Pile 4).

The coherent pile force/moment diagrams with depth are plotted with black line, while the incoherent pile diagrams are plotted with red lines (thick line for mean value and thin lines for the 20 samples). Figures 10 also includes results obtained for the inclined S-P incident waves with 15 and 30 degrees incidence angle with vertical direction. The wave inclination effects are minor for the pile forces and moments.

From Figure 10, it should be noted that the motion incoherency increases the pile maximum bending moments by about 15% at lower depth under basemat and also increases the pile maximum axial forces by up to 30% for the peak-bearing piles at large depths close to the rock formation.

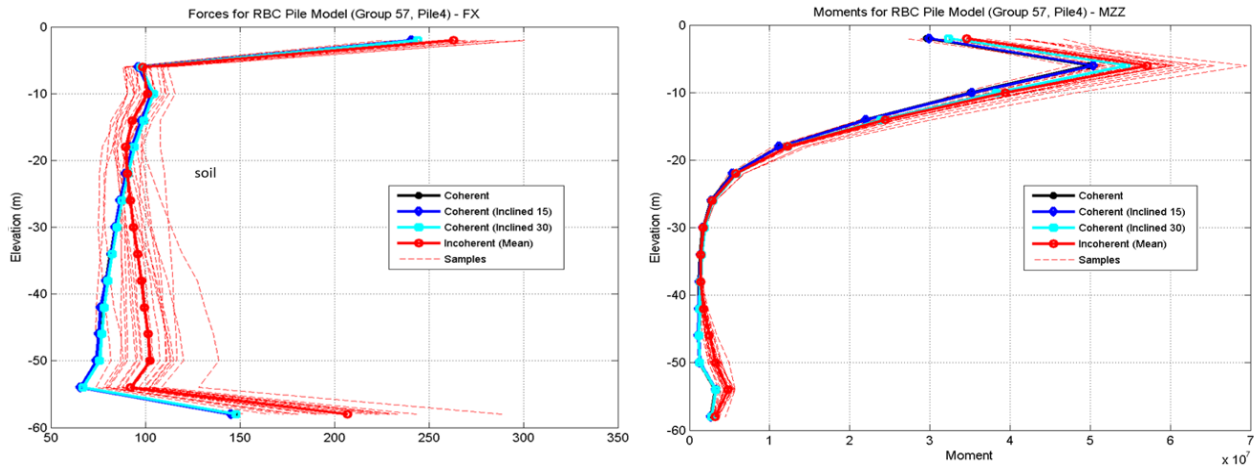


Figure 10 Coherent vs. Incoherent Pile Maximum Axial Forces (left) and Bending Moments (right)

### NONLINEAR SOIL BEHAVIOR EFFECTS

In this section, the effects of the local hysteretic soil material behaviour in the vicinity of piles is investigated. Only the peak-bearing piles is considered. The local nonlinear soil behaviour was modelled using an iterative equivalent-linearization procedure, in principle similar with the procedure included the SHAKE code for the 1D layered soil models (Idriss and Sun, 1992). However, the local nonlinear soil behaviour effects in the 3D soil space of the FE model, the shear modulus and damping soil material curves are considered as functions of the local maximum octahedral shear strain computed in each soil element.

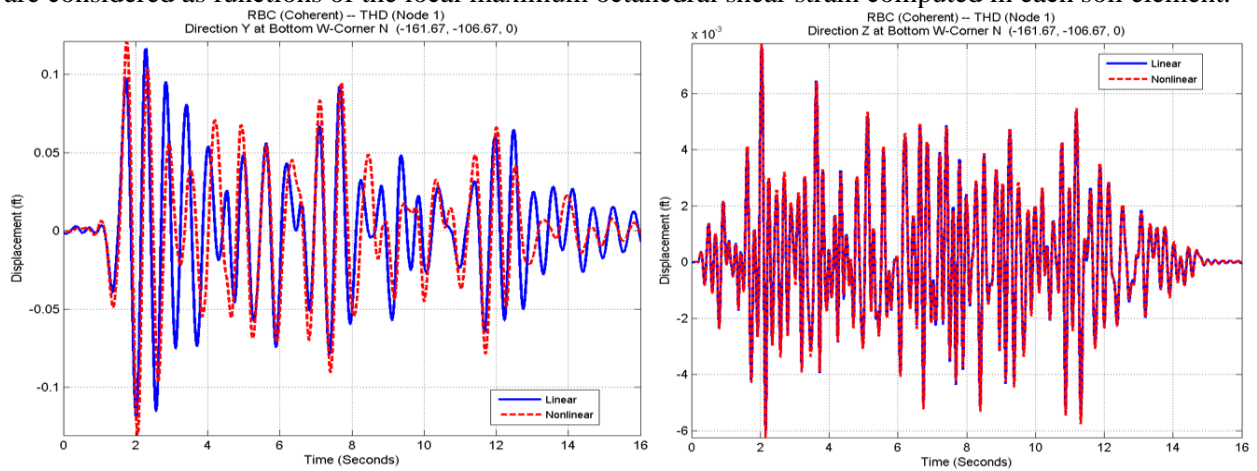


Figure 11 Linear vs. Nonlinear Relative Displacement at the Basemat Level for Y and Z directions

After each linearized SSI analysis iteration, to avoid making linear superpositions that will be incorrect for nonlinear analysis, the octahedral shear strains computed for each input direction, X, Y and Z are combined

before considering the hysteretic soil behaviour for each soil element. This iterative equivalent-linearization SSI analysis is performed automatically in ACS SASSI (Ghiocel, 2019).

Figures 11 and 12 show the relative nonlinear displacements of basemat and high-elevation locations of the RB complex with respect to the free-field motion. The nonlinear hysteretic soil behaviour amplifies the horizontal displacement response and produces no effect on the vertical displacement response.

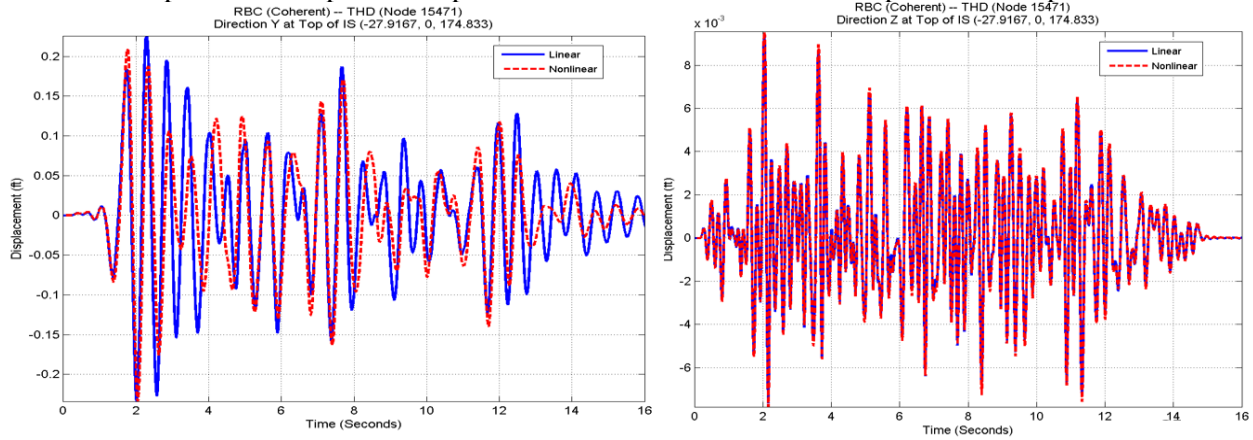


Figure 12 Linear vs. Nonlinear SSI Relative Displacements at High-Elevation Level for Y and Z directions

Figures 13 through 15 show in detail the nonlinear soil behaviour in the vicinity of piles. Figure 13 shows that the nonlinear soil maximum shear strains are large in the vicinity of the piles up to 0.50% strain. Figure 14 shows the iterated effective shear modulus values in vicinity of piles, and Figure 15 shows the iterated effective damping in vicinity of piles. Three iterations were sufficient for nonlinear response convergence.

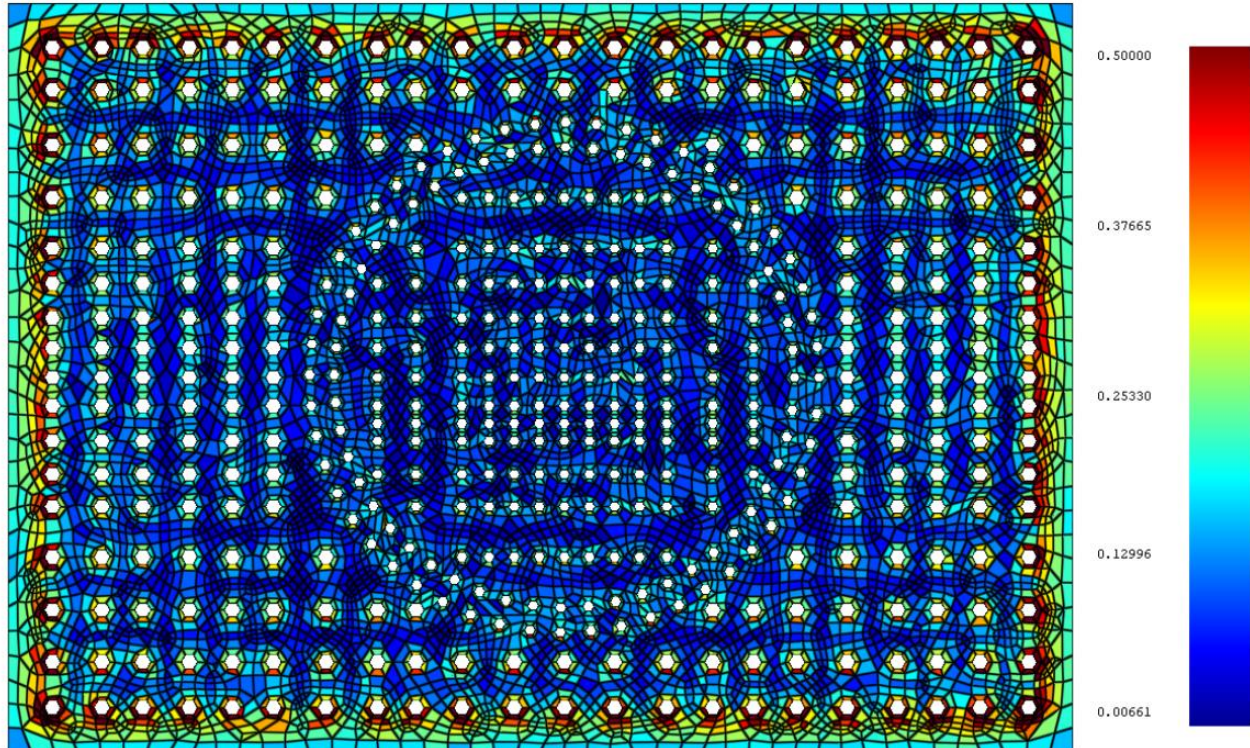
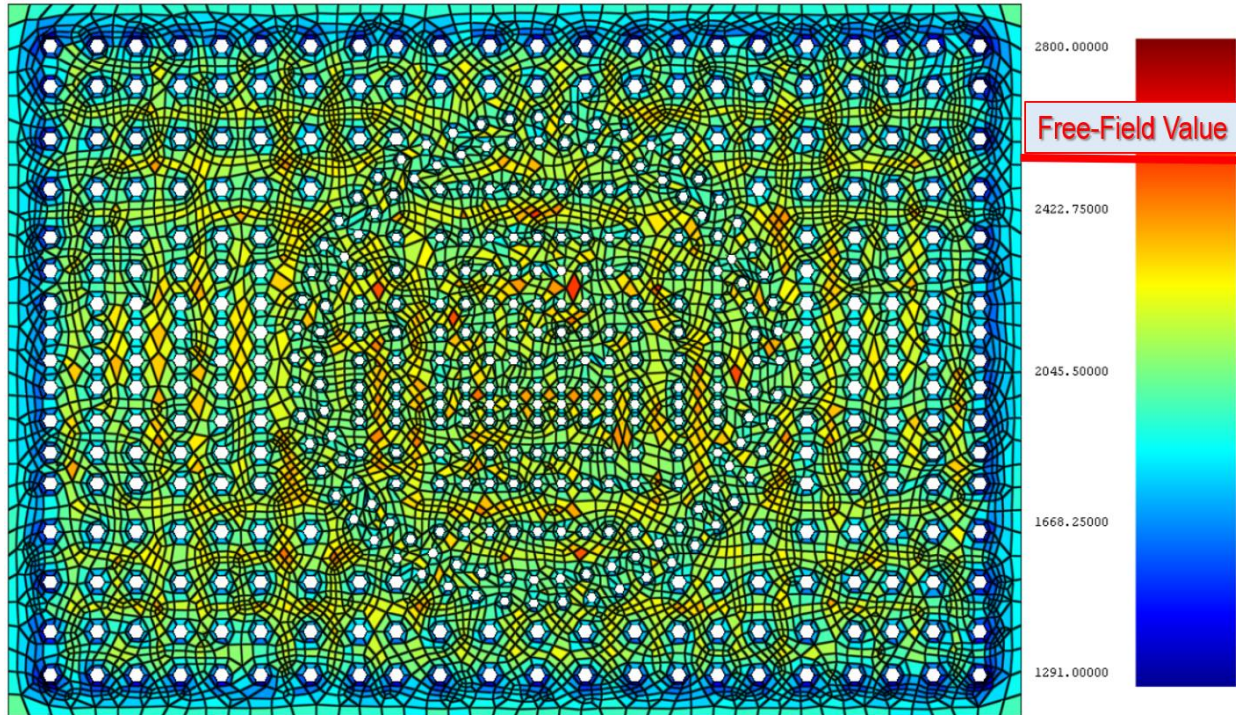
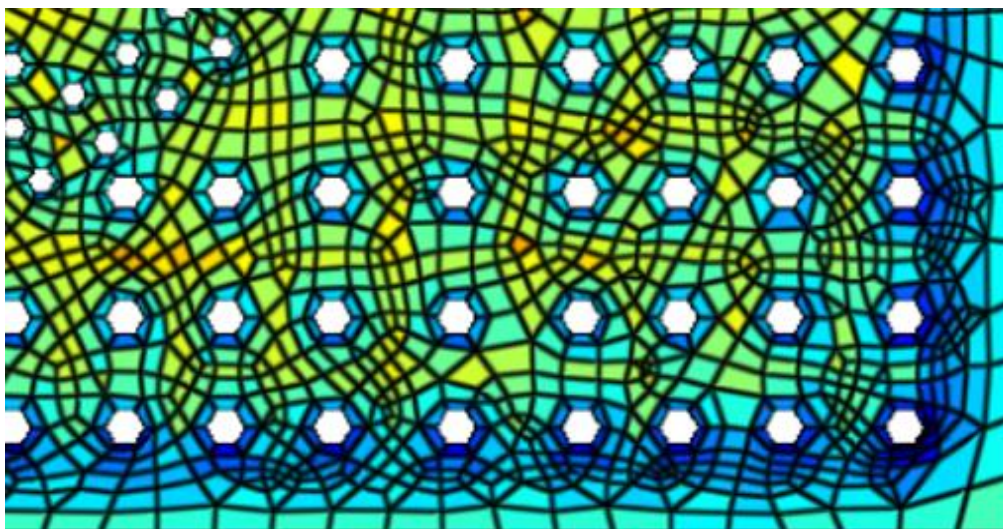


Figure 13 Maximum Soil Octahedral Shear Strain in Vicinity of Piles

It should be noted the significant nonlinear soil behaviour in the vicinity of each internal pile, but also at the boundary between the entire pile foundation and the far-field soil. The largest soil strain values of 0.50 are noted at the pile foundation external boundary. This indicates that the entire foundation is moving as a large embedment foundation within the soil deposit. Also, the soil strain values indicates the effect of the RB complex rocking motion that increases local soil strains for piles larger closer to foundation edges. The soil strain values directly affect the soil shear stiffness and damping for soil elements adjacent to the piles.



a) Entire Pile Foundation Layout

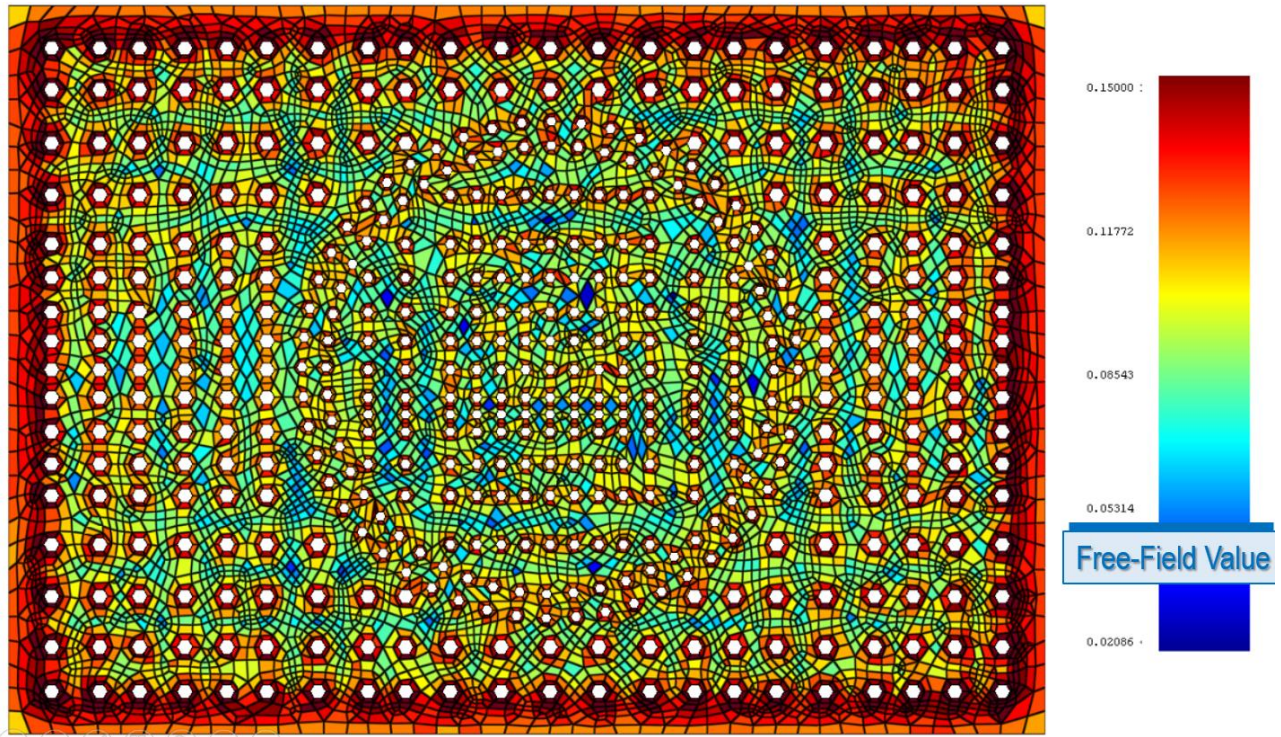


b) Zoomed Lower-Right Corner of Pile Foundation

Figure 14 Effective Shear Modulus in Vicinity of Piles

Figure 14 shows the effects of the nonlinear soil behaviour on the soil stiffness near piles. The soil shear modulus decreases from 2,500 ksf in the far-field soil down to a local shear modulus value of 2,000 ksf for

the inter-pile soil elements, and 1,300 ksf for the pile-foundation external boundary soil elements. Figure 15 shows the effects of the nonlinear soil behaviour on the soil material damping near piles. The soil damping ratio values vary from the 3% value in the far-field up to 15% for the inter-pile soil elements, and 18% for the pile-foundation external boundary soil elements.



a) Entire Pile Foundation Layout



b) Zoomed Lower-Right Corner of Pile Foundation

Figure 15 Iterated Effective Shear Modulus in Vicinity of Piles

Although the nonlinear soil behaviour near piles affects only negligible the global foundation within the soil as shown in Figures 10 and 11, it is expected that the larger increase in the soil damping near piles will affect the in-structure responses.

From Figures 16 and 17 show the ISRS computed at the basemat corner (elevation 0 ft) and at a high elevation (elevation 111.65 ft). It should be noted that the SSI dominant mode ISRS spectral peak @ 1.9 Hz is largely reduced due to the nonlinear soil behaviour for both horizontal and vertical directions. It is also remarked that the nonlinear soil behaviour produces a shift of the SSI dominant ISRS spectral peak from @ 1.9 Hz to @ 1.6 Hz. This ISRS spectral peak reduction is visible in all three figures.

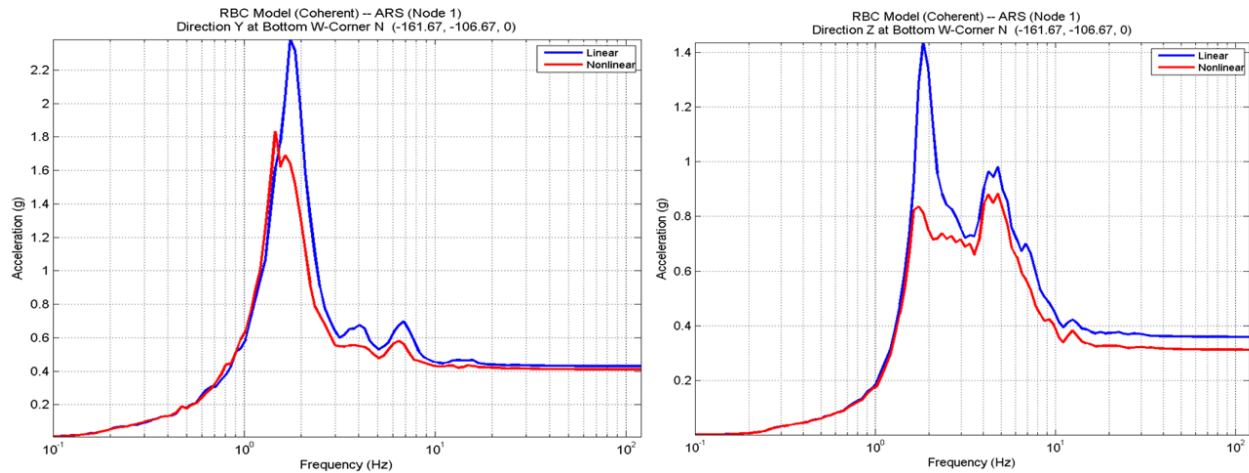


Figure 16 ISRS for Linear vs. Nonlinear Soil Behaviour at the Basemat Level for Y and Z directions.

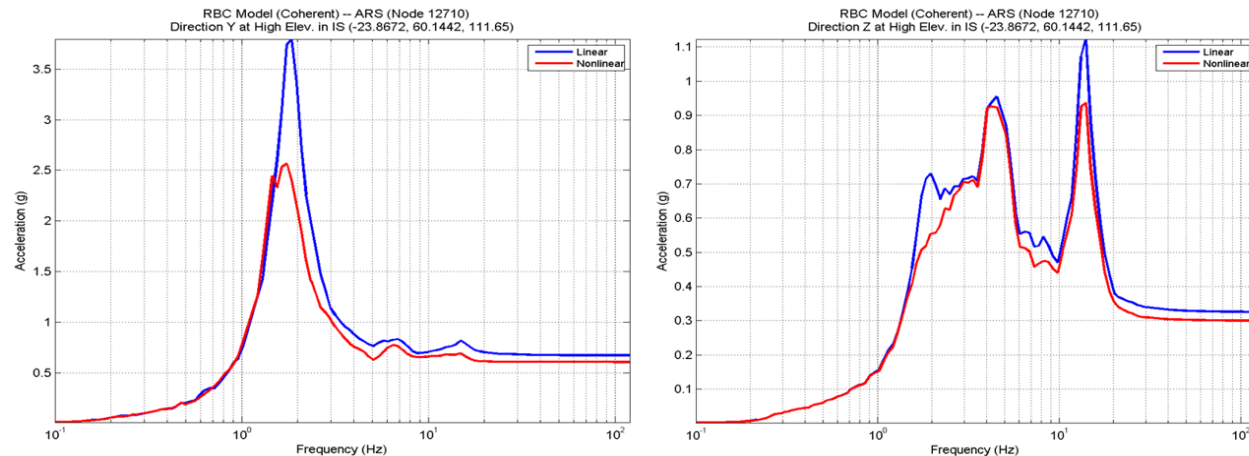


Figure 17 ISRS for Linear vs. Nonlinear Soil Behaviour at High Elevation 111.65 ft for Y and Z directions

Figures 18 shows the effects of the nonlinear soil behaviour on the pile maximum axial forces and bending moments for the foundation corner pile marked in Figure 2.

From the Figure 18 plots, it should be noted that the soil nonlinear behaviour reduces the seismic axial forces in piles, most likely as a result of reducing the building accelerations and the vertical seismic loads on piles. Due to the nonlinear soil behaviour that produces a soil stiffness reduction, the pile bending moments increase in the middle of piles, and slightly decrease at the top and bottom of the piles.

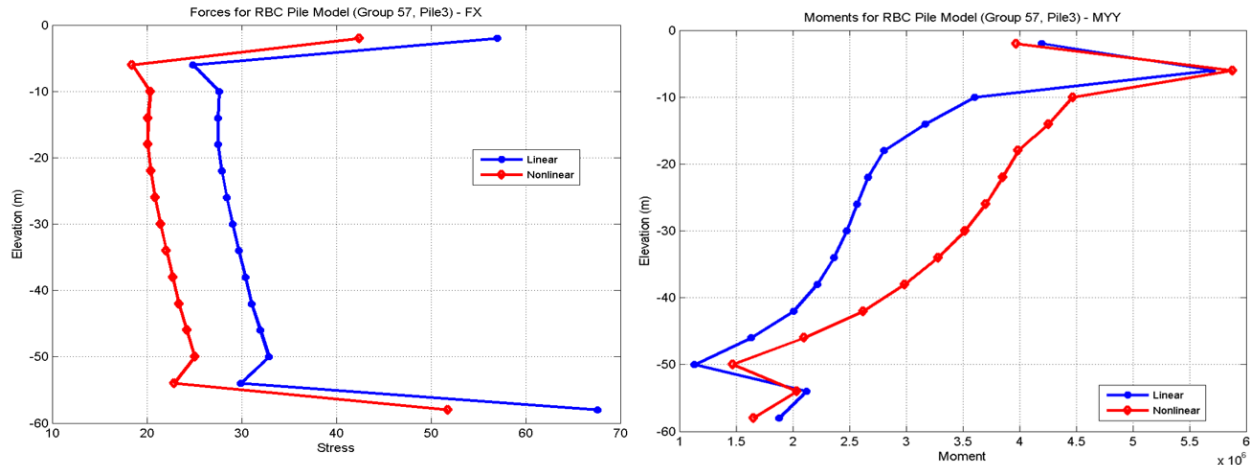


Figure 18 Corner Pile Maximum Axial Forces and Bending Moments for Linear vs. Nonlinear Soil

## CONCLUDING REMARKS

Using an efficient SSI methodology based on an iterative equivalent-linearization numerical procedure, the paper investigates the effects of nonlinear soil behaviour on the seismic SSI response of RB complex on piles. The nonlinear hysteretic soil behaviour in the vicinity of the piles significantly reduces the RB complex ISRS mainly due to the large increase in the local soil material damping in the vicinity of piles.

As a general conclusion for practice is that using the standard linearized SASSI methodology for the heavy buildings on piles provides a conservative, possibly overly conservative, approach for computing the ISRS, and the forces and moments in structure and piles. The SSI effects of the increased soil damping near piles is to reduce structural accelerations and by this to also decrease all other seismic responses.

The motion incoherency effects are less significant since the SSI system is a low frequency oscillating system. However, the motion incoherency can slightly increase the pile axial forces and bending moments.

## REFERENCES

- Abrahamson, N. (2007). *Effects of Spatial Incoherence on Seismic Ground Motions*, Electric Power Research Institute Report No. TR-1015110, Palo Alto, CA and US Department of Energy, Germantown, MD, December 20
- Ghiocel, D. M. (2019). *Sensitivity Studies for Nuclear Island Founded on Piles Including Effects of Seismic Motion Spatial Variation and Local Nonlinear Behaviour*, SMiRT25 Conference, Division 3, Charlotte, NC, August 4-9
- Ghiocel, D. M. (2022). *Efficient Linear and Nonlinear Seismic SSI Analysis of Deeply Embedded Structures Using Flexible Reduced-Order Modeling (FVROM)*, SMiRT26 Conference, Div. 5, Berlin/Potsdam, Germany, July 10-15
- GP Technologies (2019). “ACS SASSI - An Advanced Computational Software for 3D Dynamic Analyses Including SSI Effects”, *ACS SASSI V4 User Manuals, Revision 0*, Rochester, New York
- Nie, J., Braverman, J., and Costantino, M. (2013). “Seismic Soil-Structure Interaction Analyses of A Deeply Embedded Model Reactor – SASSI Analyses”, *U.S. Department of Energy, Brookhaven National Laboratory, BNL 102434-2013*, New York
- Idriss I.M, Sun J.I (1992) “SHAKE 91: A Computer Program for Conducting Equivalent Linear Seismic Response Analyses of Horizontally Layered Soil Deposits”, *Technical Report at Department of Civil Engineering, University of California, Davis*